AD_______________

Award Number: W81XWH-08-1-0503

TITLE: Noninvasive Subharmonic Pressure Estimation for Monitoring Breast Cancer Response to Neoadjuvant Therapy

PRINCIPAL INVESTIGATOR: Flemming Forsberg, Ph.D.

CONTRACTING ORGANIZATION: Thomas Jefferson University
Philadelphia, PA 19107

REPORT DATE: January 2013

TYPE OF REPORT: Final

PREPARED FOR: U.S. Army Medical Research and Materiel Command
Fort Detrick, Maryland 21702-5012

REPORT DOCUMENTATION PAGE

Form Approved
OMB No. 0704-0188

1. REPORT DATE
January 2013

2. REPORT TYPE
Final

3. DATES COVERED
1 September 2008 – 31 December 2012

4. TITLE AND SUBTITLE

Noninvasive Subharmonic Pressure Estimation for Monitoring Breast Cancer Response to Neoadjuvant Therapy

5a. CONTRACT NUMBER

5b. GRANT NUMBER
W81XWH-08-1-0503

5c. PROGRAM ELEMENT NUMBER

6. AUTHOR(S)

Flemming Forsberg, Ph.D.

E-Mail: flemming.forsberg@jefferson.edu

5d. PROJECT NUMBER

5e. TASK NUMBER

5f. WORK UNIT NUMBER

7. PERFORMING ORGANIZATION NAME(S) AND ADDRESS(ES)

Thomas Jefferson University
Philadelphia, PA 19107

8. PERFORMING ORGANIZATION REPORT NUMBER

9. SPONSORING / MONITORING AGENCY NAME(S) AND ADDRESS(ES)
U.S. Army Medical Research and Materiel Command
Fort Detrick, Maryland 21702-5012

10. SPONSOR/MONITOR'S ACRONYM(S)

11. SPONSOR/MONITOR'S REPORT NUMBER(S)

12. DISTRIBUTION / AVAILABILITY STATEMENT
Approved for Public Release; Distribution Unlimited

13. SUPPLEMENTARY NOTES

14. ABSTRACT

Please see next page.

15. SUBJECT TERMS
Breast Cancer, Ultrasound Imaging, Ultrasound Contrast Agent, Pressure Estimation, Neoadjuvant chemotherapy

16. SECURITY CLASSIFICATION OF:			17. LIMITATION OF ABSTRACT	18. NUMBER OF PAGES	19a. NAME OF RESPONSIBLE PERSON
					USAMRMC
a. REPORT	b. ABSTRACT	c. THIS PAGE			19b. TELEPHONE NUMBER *(include area code)*
U	U	U	UU	33	

13. ABSTRACT *(Maximum 200 Words)*

Neoadjuvant chemotherapy is currently the standard of care for locally advanced breast cancer (LABC). Monitoring tumor response is advantageous for patients. This project aims at establishing noninvasive monitoring of neoadjuvant chemotherapy in the breast using subharmonic aided pressure estimation (SHAPE) to estimate the interstitial fluid pressure (IFP) in LABC. *In vitro* experiments with the ultrasound contrast agent Definity have showed an inverse linear relationship between the change in subharmonic amplitude and hydrostatic pressure (r^2=0.63-0.95, $p<0.01$) over the pressure range associated with breast tumors (0–50 mmHg). *In vivo* proof of concept for SHAPE as a noninvasive monitor of IFP (r^2=0.67-0.96, $p<0.01$) has been provided based on a swine model. The work on *in vivo* SHAPE measurements of IFP was selected for the final of the American Institute of Ultrasound in Medicine (AIUM) 2011 Young Investigator Award (for VG Halldorsdottir) and was awarded **FIRST** place out of 90 abstracts submitted for this competition. In total, 97 female, nude rats were implanted with MDA-MB-231 cells and 51 animals were successfully studied with SHI and SHAPE 21, 24 or 28 days after tumor inoculation. However, the comparisons between SHAPE and Stryker IFP measurements have yet to be completed. The SHI images of tumor vascularity were compared to immunohistochemical markers of angiogenesis (CD31, COX-2 and VEGF). The strongest correlation determined by linear regression in this breast cancer model was between SHI and percent area stained with VEGF (r=0.53).

3 TABLE OF CONTENTS

3 TABLE OF CONTENTS 3
4 INTRODUCTION 4
5 BODY 5
5.1 Methods 6
5.2 Results and Discussion 11
6 KEY RESEARCH ACCOMPLISHMENTS 18
7 REPORTABLE OUTCOMES 19
8 CONCLUSIONS 26
9 REFERENCES 27
Appendix I 31

4 INTRODUCTION

In the United States, close to 5 – 20 % of newly diagnosed breast cancer and 10 – 30% of all primary breast cancer is diagnosed as locally advanced breast cancer (LABC) [1, 2]. Neoadjuvant chemotherapy (systemic preoperative chemotherapy) is currently the standard of care for LABC [3, 4]. When compared with adjuvant chemotherapy (postoperative therapy), neoadjuvant chemotherapy yields similar results for both overall survival (70% for both) and disease-free survival (53% adjuvant, 55% neoadjuvant) [5]. Thus, the postponement of surgery does not affect the outcome of the treatment [5, 6]. In addition, neoadjuvant chemotherapy offers considerable benefits to the patient as the treatment can shrink the tumor and even in some cases offer complete pathologic response [3, 7]. This reduction in tumor size increases the possibility of breast conservation [3, 5-7]. Maximizing the conservation of breast tissue can be of great personal importance for the self-esteem and quality of living of the patient [6]. Neoadjuvant chemotherapy can also offer an early indication of the patient's response to chemotherapy. Consequently, monitoring tumor response to neoadjuvant therapy gives the possibility of adjusting the treatment if the patient is responding poorly or not at all resulting in substantial advantages for the patient [3, 6]. This project aims at establishing noninvasive monitoring of neoadjuvant chemotherapy in the breast using subharmonic aided pressure estimation (SHAPE; U.S. Patent 6,302,845).

Generally interstitial fluid pressure (IFP) is 10-30 mmHg higher in cancerous tissue than in normal tissue although values of up to 60 mmHg have been recorded [8, 9]. Similarly, IFP in breast cancer tumors has been shown to be higher than that of surrounding breast tissue [9]. This increase is believed to be due to vascularity, fibrosis and difference in the interstitial matrix in tumors and it can result in poor transport of therapeutic drugs to tumors [8]. Taghian et al. used a wick-in-needle technique to monitor the IFP of breast cancer before and after neoadjuvant chemotherapy with two drugs used consecutively [10]. When used as a first drug Paclitaxel decreased the IFP by 36% ($p=0.02$) whereas with Doxorubicin as a first drug there was only 8% reduction ($p=0.41$). As this was a hypothesis-generating study they did not show any outcome related to the relationship between IFP and therapy response [10]. However, the level of IFP has been shown to predict disease free survival for cervix cancer (34% disease free survival (DFS) if IFP > 19 mmHg, 68% DFS if IFP < 19 mmHg ($p = 0.002$)) [11]. Thus, the level of interstitial fluid pressure (IFP) in breast cancer tumors could potentially be used to monitor the response to neoadjuvant chemotherapy.

Contrast agents have been used for two decades to improve visualization in ultrasound (US) imaging as they enhance the difference in reflectivity between tissues [12]. Because of the difference in compressibility between the medium and the microbubble any changes in pressure induce changes in the size of the microbubble [13]. This in turn affects the reflectivity and resonant frequency of the bubble [13, 14]. In subharmonic imaging (SHI) pulses are transmitted at a frequency f_0 and the echoes are received at half that frequency $f_0/2$. SHI has been showed to be a feasible option for contrast enhanced imaging due to subharmonic generation by contrast agents and limited subharmonic generation in tissues [15]. Our group came up with a novel technique, SHAPE, utilizing microbubbles and the subharmonic amplitude of the scattered signal [13]. We showed that there is a linear relationship between the hydrostatic pressure and the subharmonic amplitude. We propose the use of SHAPE to monitor treatment response by noninvasively measuring the IFP in breast tumors. This offers several benefits to the patient. As opposed to the wick-in-needle technique SHAPE is noninvasive and does not inflict pain. Furthermore, it allows for an early indication of responders vs. non-responders and thereby makes adjustments to therapy easier. Moreover, SHAPE has been shown to have a favorable signal-to-noise ratio so the subharmonic amplitude is not affected by background noise [13].

The optimal contrast agent and acoustic parameters for SHAPE will be established using *in vitro* pulse-echo measurements. The SHAPE algorithm will then be designed and implemented on a commercial, state-of-the-art US scanner for *in vivo* IFP measurements. A similar algorithm has already been set up for cardiac SHAPE and thus only a few adjustments need to be made to implement SHAPE for breast tumors making this very cost-effective. The *in vivo* experiments will be twofold. First, athymic, nude, female rats will be implanted with SKBR3, MCF-7 or BT474 human breast cancer cells and SHAPE used to measure IFP and calibrated by comparing the SHAPE results to IFP measurements obtained with an invasive, intra-compartmental pressure monitor as the gold standard. After calibration, human xenograft breast tumors in athymic, nude, female rats will be used to evaluate the ability of SHAPE to track changes in IFP by studying before and after administration of a chemotherapy agent (paclitaxel).

Our group has proposed that SHAPE and contrast enhanced US imaging can be used to measure the IFP in LABC tumors, thus, making it possible to noninvasively monitor the tumor response to neoadjuvant chemotherapy. This method would be a considerable improvement from the wick-in-needle technique currently used for IFP measurements in LABC and allow for individualized treatments options.

5 BODY

The hypothesis of this project is that IFP in breast tumors can be measured noninvasively using SHAPE and contrast enhanced US thus improving the monitoring of neoadjuvant chemotherapy. To investigate this prospect, *in vitro* pulse-echo experiments will be conducted to investigate this prospect and find the optimal contrast agent for SHAPE. These results will then be used to implement SHAPE on a commercial scanner. The scanner will be used for *in vivo* studies on 201 rats with tumor xenografts in order to calibrate and evaluate SHAPE's ability to monitor response to neoadjuvant chemotherapy. The specific tasks of the project (as presented in the original Statement of Work) can be found in Appendix I.

First an outline of the methods applied will be given followed by a presentation of the results to date. Finally, the conclusions and future directions of the research will be discussed.

5.1 Methods

In vitro experiments

A pulse-echo system, similar to the one previously developed by our group [13], was constructed to test different types of contrast agents for use with high frequency SHAPE. A programmable function generator (8116A; Hewlett Packard, Santa Clara, CA) produced pulses, which were supplied to the transmit transducer after amplification in a broadband 50 dB RF power amplifier (325LA; ENI, Rochester NY). Received microbubble signals were amplified with a low noise RF amplifier (5052 PR; Panametrics, Waltham, MA), digitized and processed (with the built-in FFT function) using a digital oscilloscope (9350AM; LeCroy, Chestnut Ridge, NY). The amplitude of the harmonic and subharmonic signal components was obtained from spectra averaged over 64 sequences. Command delivery and data transfer was controlled by LabView (National Instruments, Austin, TX). The subharmonic amplitude at different static pressures was measured using a sealed water tank capable of withstanding pressure changes over 200 mmHg. Single element transducers with center frequencies of 4 to 12 MHz were used as transmitter and receiver. The tank was immersed in a water bath at room temperature (25°C). The pressure inside the tank was monitored by a pressure gauge (OMEGA Engineering, Stamford, CT). An inlet and an outlet on the tank were constructed for injecting microbubbles and for applying extra hydrostatic pressure.

In order to find the optimal contrast agent for high-frequency SHAPE changes in the amplitudes of the first, second and subharmonic were measured for two different contrast agents; Definity (Lantheus Medical Imaging, N Billerica, MA) and Sonazoid (GE Healthcare, Oslo, Norway) at pressures from 0 to 47 mmHg (to simulate the IFP in breast tumors). Furthermore, the frequency and acoustic pressure were varied from 5.7 to 9.3 MHz and 0.7-1.2 MPa, respectively, to determine the optimal acoustic parameters. After data retrieval the amplitude of the first, second and subharmonic was extracted using MATLAB (Mathworks, Natick, MA). Three measurements were acquired at each setting and linear regression analysis used to determine the relationship between hydrostatic pressure and change in amplitude for the first, second and subharmonic. All statistical analysis was conducted using Stata 12.0 (Stata Corporation, College Station, TX).

Two alternative *in vitro* approaches were also investigated. First, we repeated the static pressure measurements using a different – potentially more suitable - water tank. Small (10 ml) OptiCell chambers (Nunc, Rochester, NY) have been used successfully to investigate interactions between contrast bubbles, ultrasound and cancer cells [16] and these were, therefore, selected as the new container for static pressure tests. The OptiCell was submerged into a larger water tank and 0.2 ml/l of Definity (Lantheus Medical Imaging, N Billerica, MA) injected. RF signals were acquired with a Sonix RP ultrasound scanner (Ultrasonix, Richmond, BC, Canada) using a high frequency, linear array and compared to an invasive (needle-in-wick) pressure monitor (Stryker, Berkshire, UK) as the reference standard. A 2.5 cm tissue mimicking phantom was placed between the probe and the OptiCell chamber to simulate tissue attenuation. Two different transmit frequencies of 6.7 and 10 MHz were considered. Contrast echoes were received at half the transmit frequencies (i.e., 3.35 and 5.0 MHz). The acoustic parameters were varied and the amplitude of the subharmonic signal component was extracted and analyzed as described above.

Secondly, a completely new tank (with extra acoustic absorbers incorporated to minimize reverberations) was designed. The new water tank was constructed and the pressure inside the tank was monitored by a pressure gauge (OMEGA Engineering, Stamford, CT; Fig 1). A state-of-the-art commercial scanner Sonix RP (Ultrasonix Medical Corporation, Richmond, BC, Canada) with a high frequency linear array (L14-5/38) was used to acquire radio-frequency (RF) data at the focal zone depth (4.25 cm) at a 9 Hz framerate following injection of the contrast agent Definity (Lantheus Medical Imaging, N Billerica, MA) in a 0.2 ml/l dose. Two different transmit frequencies of 6.7 and 10 MHz were considered. Contrast echoes were received at half the transmit frequencies (i.e., 3.35 and 5.0 MHz). The acoustic output power was varied from 0 to -20 dB (in 2 dB steps; 0.24-2.05 MPa) for a 0 mmHg hydrostatic pressure in order to establish the optimal sensitivity for SHAPE. Then the chamber pressure was varied from 0 to 50 mmHg to simulate IFP in tumors and acoustic pressure varied from -16 to -4 dB (in 4 dB steps). After RF data acquisition, files were transferred to a PC and the amplitude of the subharmonic signal component was extracted using MATLAB (Mathworks, Natick, MA) as shown in Figure 2. Three measurements were acquired at each setting and linear regression analysis used to determine the relationship between hydrostatic pressure and change in subharmonic amplitude. All statistical analyses were conducted using Stata 9.0-12.0 (Stata Corporation, College Station, TX).

Moreover, a novel, simulation model of the dynamics of an encapsulated microbubble contrast agent, developed as part of a previous DOD supported project [14], was modified in order to account for ambient pressure variations and different shell parameters to establish the optimal contrast microbubble for SHAPE. A nonlinear extension of the original viscoelastic model was pursued by considering a quadratic elasticity model where the interfacial elasticity vary linearly with area fraction as well as an exponential model (i.e., the elasticity vary exponentially).

Figure 1. *The re-designed water tank scanned by the L14-5 transducer. Notice the digital pressure gauge on the top of the tank.*

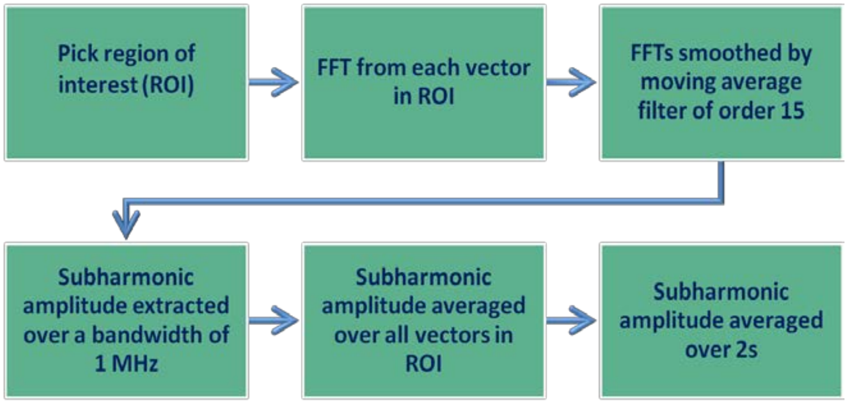

Figure 2. *Block diagram of the off-line processing performed on the RF data.*

In vivo experiments

All research studies involving animals were approved by the Institutional Animal Care and Use Committee of Thomas Jefferson University and conducted in accordance with the guidelines provided by the National Institutes of Health.

Our group has worked in partnership with Ultrasonix Medical Corporation to implement SHAPE for cardiac use on a state-of-the-art commercial scanner Sonix RP (Ultrasonix Medical Corporation, Richmond, BC, Canada) with a phased array (PA4-2). Several experiments have been carried out in canines to investigate cardiac SHAPE supported by funding from the AHA and the NIH. RF data from these experiments was analyzed off-line using Matlab. The software developed by our group for this analysis is not site-specific and will also be used to analyze the data we will acquire from *in vivo* breast SHAPE in rats as part of this project.

Furthermore, an opportunity to provide a proof-of-concept of the use of SHAPE for estimating IFP and test the invasive (needle based) Stryker pressure monitoring system (the reference standard) presented itself. As part of an ongoing NIH study, a unique, naturally occurring tumor model, the Sinclair swine with melanoma, was being studied. We obtained IFP measurements from the tumors and surrounding tissue using the Stryker needle based system, which provided us with a chance to assess the dependence of this technique on the angle between the needle and the tissue. Moreover, subharmonic signals were acquired during an infusion of Definity (6.25 ml/l/min) with the Sonix RP and a linear array. Data were obtained at 6.7 and 10 MHz (i.e., subharmonic frequencies of 3.75 and 5.0 MHz, respectively) with acoustic outputs of -4, -8 and -12 dB and analyzed further during the last year. Five (5) swine were studied (one melanoma per swine) at no cost to this project.

Originally, we planned to study three human breast cancer cell lines SKBR3, MCF-7 and BT474 in this project. However, our collaborators advised us against trying to work with so many different cell lines in the short time available for the *in vivo* rat experiments. Hence, it was decided to focus our efforts on the MDA-MB-231 breast cancer cell line, since it is known to grow successfully in rats [17-19]. This cell line was also selected, because it is able to upregulate intracellular pH to near normal levels and, therefore, have a higher likelihood of remaining viable under the adverse (low pH) conditions that are typical of the tumor microenvironment [20]. Cells in such an environment are the most stimulatory in terms of inducing tumor angiogenesis. The MDA-MB-231 cell line was cultured in Eagle's Minimum Essential medium alpha modification (alpha MEM; Sigma-Aldrich Co., St. Louis, MO) in an incubator at 37º C with a 5 % CO_2 in air atmosphere.

Female, 5-8 weeks old, nude, athymic rats (Charles River Laboratories, Wilmington, MA), weighing between 150 and 250 g, were injected subcutaneously with approximately 5 x 10^6 tumor cells into the right mammary fat pad. However, it took almost 8 months to arrive at a stable and consistent level of cell growth for the MDA-MB-231 cells, which also produced tumor growth *in vivo*. Twelve (12) rats were evaluated in this period and our studies indicated that time points of 21, 24 or 28 days after tumor inoculation ensured enough difference in tumor volume and tumor vasculature for effectively monitoring the progression of angiogenesis

For the SHAPE experiments, it is critical to select the appropriate acoustic output (AO) power (i.e., in the growth phase of the subharmonic signal generation). Hence, our group developed an automated AO optimization algorithm to identify the AO level eliciting growth stage subharmonic signals to help eliminate the problems of acquiring and analyzing the data offline at all AO levels (as in our previous studies) [21]. The AO optimization algorithm was implemented on a Sonix RP scanner along with pulse inversion SHI transmitting at 8 MHz and receiving at 4 MHz. The optimization algorithm stepped the ultrasound scanner from 0 to 100 % AO. A logistic equation fitting function was applied with the criterion of minimum least squared error between the fitted subharmonic amplitudes and the measured subharmonic amplitudes as a function of the AO levels and the optimum AO level was chosen corresponding to the inflection point calculated from the fitted data (Fig. 3).

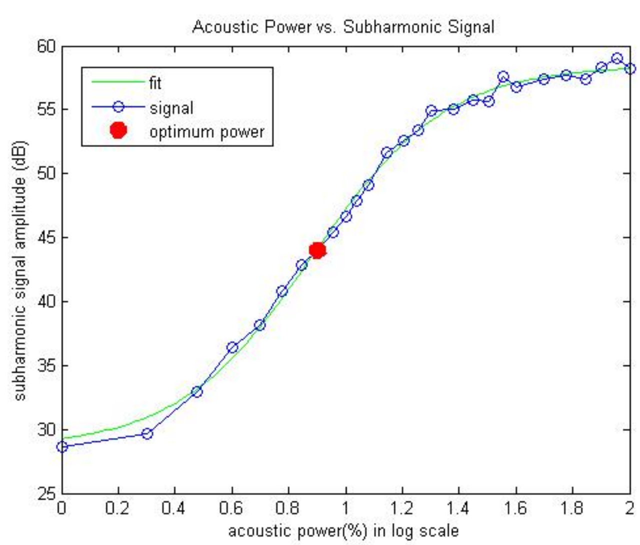

Figure 3. *Example of the outcome of the AO optimization algorithm.*

For the initial calibration studies, 25 rats received MDA-MB-231 cell line implantations. The IFP of the normal mammary fat pad as well as the tumor was measured with an intra-compartmental pressure monitor (selected as the reference standard technique for this study). The Stryker pressure monitor is an accurate but invasive technique for sampling the interstitial fluid and measuring the IFP. Grayscale SHI was performed with the modified Sonix RP scanner using the L14-5 linear array after contrast administration (Definity; dose: 36 μl) and the largest diameter of the tumor was imaged. Maximum intensity projections of 3 SHI measurements were constructed off-line and averaged for each SHAPE data point. Furthermore, as direct measurement of the tumor IFP using a needle based system will vary due to cancer heterogeneity, all tumor IFP data were also averaged over 3 measurements.

The remaining 60 nude rat xenografts were used to establish the ability of SHAPE to monitor therapy responses. SHAPE and the Stryker pressure monitor measurements were performed before and after administration of a single IV injection of 5 mg/kg of the chemotherapy agent paclitaxel (Mayne Pharma, Paramus, NJ) at the selected post-implantation time points. This is not similar to the therapy regimes employed in humans (which typically involve a 40 mg/kg dose), but the literature clearly describes how the human dose (even weight-based) is unsuitable for rats [22]. Hence, the choice of 5 mg/kg as the treatment dose utilized. Paclitaxel is known to reduce tumor IFP. SHAPE measurements were performed pre and 48 hours post therapy, since this is when the biggest reduction in IFP is expected. Additionally, tumor volumes were measured on days 21, 24 and 28 to allow growth curves to be established and compared. The entire study lasted no longer than 1 hour.

At the end of the US study, rats were euthanized by placing them in a gas chamber and saturating the air with CO_2. Tumors were then surgically removed and scanned *ex vivo* to identify the US imaging plane studied *in vivo*. Careful attention was paid to the labeling of each specimen by specimen-ink marking the true front, back, right and left [23]. Then specimens were placed in 10 % formalin phosphate (Fisher Scientific, Houston, TX) for 12 to 24 hours to fix all angiogenic markers, dehydrated in graded alcohols, cleaned in xylene, and embedded in paraffin using standard methods. The process of angiogenesis involves the activation, migration, and proliferation of endothelial cells [24-25]. Vascular endothelial growth factor (VEGF) is regarded as a major regulator of tumor-associated angiogenesis, since it promotes tumor growth, invasion, and metastasis [24-27]. Cyclooxygenase-2 (COX-2) is another positive regulator of angiogenesis, which is expressed in response to growth factors, tumor promoters, or cytokines [28-29]. Platelet endothelial cell adhesion molecule (PECAM or CD31) is a potent endothelial cell marker, since its expression is restricted to vascular system platelets and endothelium [30]. Each specimen was immunohistochemical stained using a monoclonal antibody against PECAM (anti-CD31; Dako Corporation, Carpinteria, CA), a polyclonal antibody against COX-2 (Santa Cruz Biotechnology, Santa Cruz, CA), and a monoclonal antibody against VEGF (Oncogene Research Products, San Diego, CA) as reference standards. Finally, the sections were mounted onto glass slides for analysis.

A semi-automated histomorphometry system incorporating a DXC-970MD color CCD camera (Sony Corporation, Tokyo, Japan) connected to an SMZ-10A microscope (Nikon, Melville, NJ, USA) was used to analyze both SHI images and specimens. The histomorphometry system employed a 4x objective and 10x ocular magnification (total magnification: 40x) to provide a digital view of each histological slide on a desktop computer [23]. Area measurements of stains and enhanced pixels relative to the total tumor area were obtained using ImagePro Plus software (Media Cybernetics, Silver Spring, MD). Briefly, the tumor was manually outlined on the images and the RGB channels used to automatically segment and count the number of enhanced or stained pixels as well as the total number of pixels within the tumor. Fractional tumor vascularity (*FV*) was calculated (in percent) as the number of contrast enhanced pixels (c_i) relative to the total number of pixels ($c_i + x_i$):

$$FV = \frac{\sum c_i}{\sum c_i + x_i} \times 100\% \tag{1}$$

Results were compared using linear regression analysis.

5.2 Results and Discussion

In vitro experiments

Over the pressure range of 0 – 50 mmHg (simulating the IFP in breast tumors) both Definity and Sonazoid showed an inverse linear relationship between the change in subharmonic amplitude and hydrostatic pressure (r^2 = 0.76–0.91, $p < 0.01$), when studied with the pulse-echo setup. These results are consistent with previous results reported by our group [13]. An example of the subharmonic amplitude for Sonazoid at 0 mmHg and 47 mmHg can be seen in Figure 4 (transmitting frequency 7.5 MHz and acoustic pressure 0.7 MPa). This process was markedly more time-consuming then originally envisaged, due to difficulty in aligning the single element transducers at these higher frequencies (compared to our original efforts e.g., in [13]) and this issue delayed the project by approximately 6 months.

As an alternative OptiCell measurements with Definity were conducted and these showed an inverse linear relationship between the change in subharmonic amplitude and hydrostatic pressure (r^2 = 0.79–0.99, $p < 0.01$). However, the decrease in subharmonic amplitudes recorded for pressure changes from 0 to 50 mmHg varied from 13.7 to 22.9 dB and 16.4 to 21.8 dB (depending on acoustic pressures) for 6.7 and 10 MHz transmission frequencies, respectively. These levels of subharmonic amplitude variation were markedly higher than our previous results obtained over a much larger pressure range (up to 200 mmHg) [13, 31-32]. After some extensive testing, we discovered that standing waves markedly influenced results and made measurements impossible to reproduce. Hence, our use of the OptiCell setup had to be abandoned and a completely new tank (with extra acoustic absorbers incorporated) had to be designed and built (as described in Section 5.1). This issue delayed the project further and we, therefore, requested and were granted a one year no cost extension.

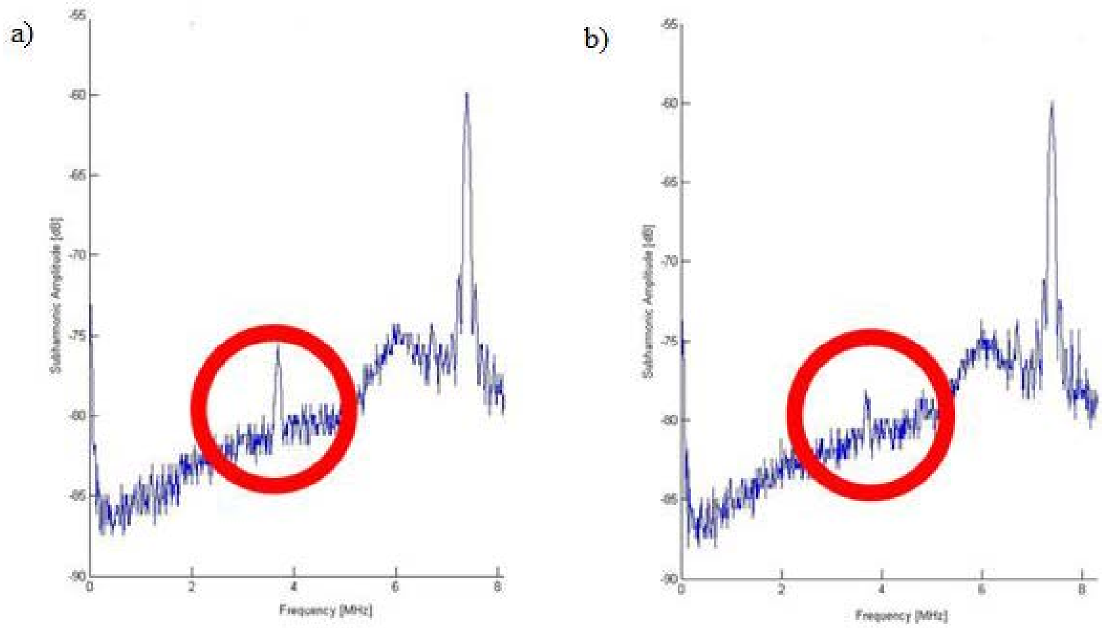

Figure 4. *Comparison of the subharmonic amplitude (circle) measured with Sonazoid at a) 0 mmHg and b) 47 mmHg pressures.*

Once the new water tank (Fig. 1) was available, we achieved much more reproducible results. The characteristic sigmoidal curve for the relationship between the subharmonic amplitude and the acoustic power showed the three stages of subharmonic generation: i.e., occurrence (-20 dB to -16 dB) where there was minimal change in the subharmonic amplitude; growth (-16 dB to - 4 dB) where there was a sharp rise in subharmonic amplitude and the subharmonic is most sensitive to pressure changes, and finally saturation (-4 dB to 0 dB) where again there is minimal subharmonic amplitude change (Fig. 5). Based on this relationship four acoustic power levels covering the growth stage and its boundaries were chosen for further investigation of hydrostatic pressure estimation using SHAPE; -16, -12, -8 and -4 dB. These values correspond to 0.33, 1.06, 1.33, 1.68 MPa and 0.24, 1.21, 1.52 and 1.78 MPa peak to peak for 6.7 MHz and 10 MHz, respectively, as measured with a 0.2 mm needle hydrophone (Precision Acoustics, Dorchester, Dorset, UK).

In the water-tank an inverse relationship was seen over a pressure change from 0 to 50 mmHg at both 6.7 MHz and 10 MHz transmission frequencies and all acoustic power levels -16 dB to -4 dB ($r^2 \geq 0.63$; $p < 0.05$; Fig. 6). The r^2 values from the linear regression analysis were consistently higher for a transmission of 10 MHz (receiving the subharmonic at 5 MHz) than for 6.7 MHz (receiving at 3.35 MHz). Moreover, pressure estimates obtained at -16 dB (start of the growth phase) showed limited sensitivity compared to the higher acoustic power settings likely due to a lack of subharmonic generation (still in the occurrence phase). The largest drop in subharmonic amplitude (corresponding to the maximum sensitivity for pressure estimation), 11.36 dB over 50 mmHg, was seen at 10 MHz and -8 dB ($r^2 = 0.95$; $p < 0.01$; Fig. 7). This is consistent with previous results reported by our group [13] and these efforts represent the fulfillment of tasks 1a, 1d, 1f, 2a and 2c in the original Statement of Work (SOW).

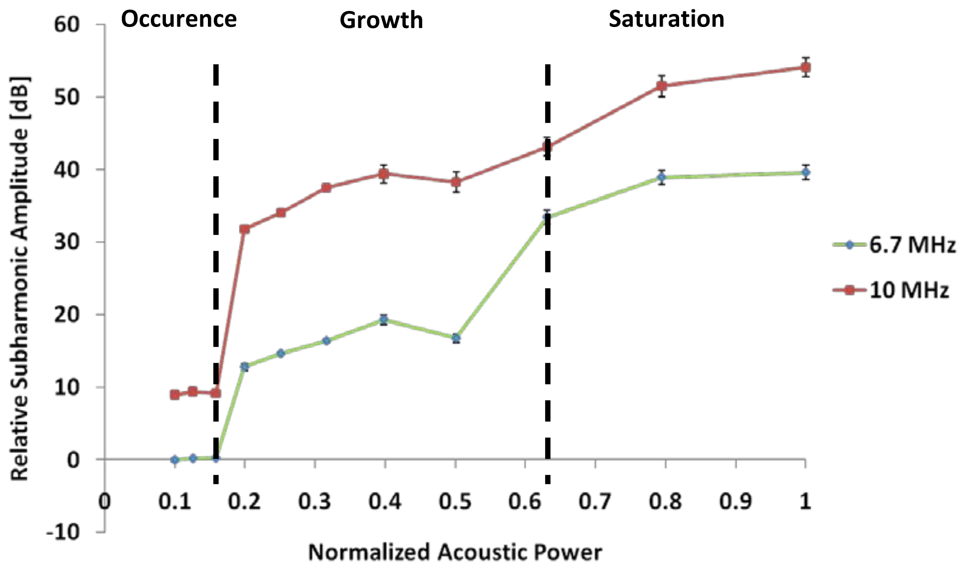

Figure 5. *Subharmonic response to changes in acoustic power with the occurrence, growth and saturation phases clearly seen.*

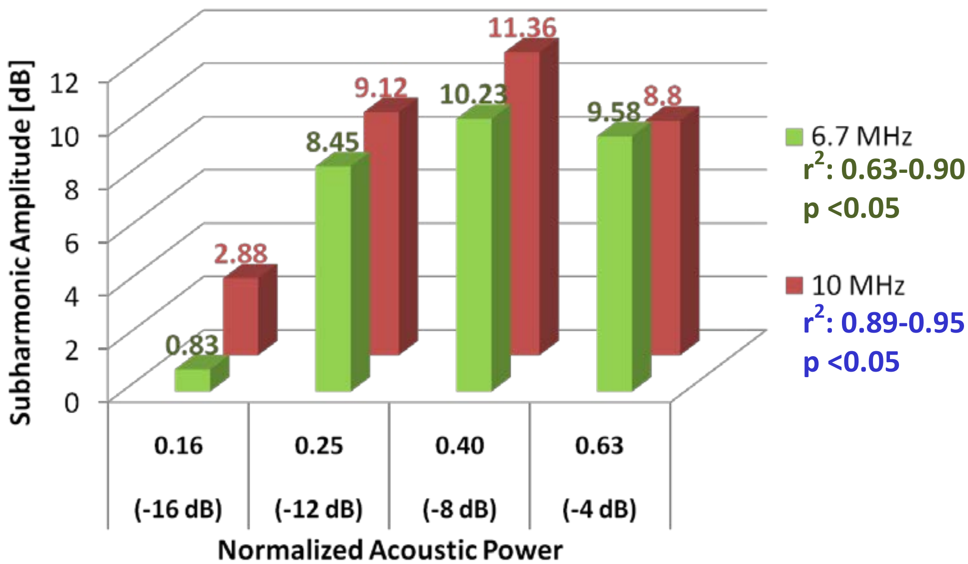

Figure 6. *Maximum decrease in subharmonic signal amplitude for Definity as a function of frequency and acoustic power (N = 3).*

The previously developed simulation model [14] was modified to include nonlinear extensions of the viscoelasticity and this model has now been published [33]. The intent was to better account for the experimentally observed changes in subharmonic signal amplitudes as a function of hydrostatic pressures. The model showed that the determining parameter of subharmonic response is the ratio of the excitation to the resonance frequency. Changing the ambient pressure changes the resonance frequency

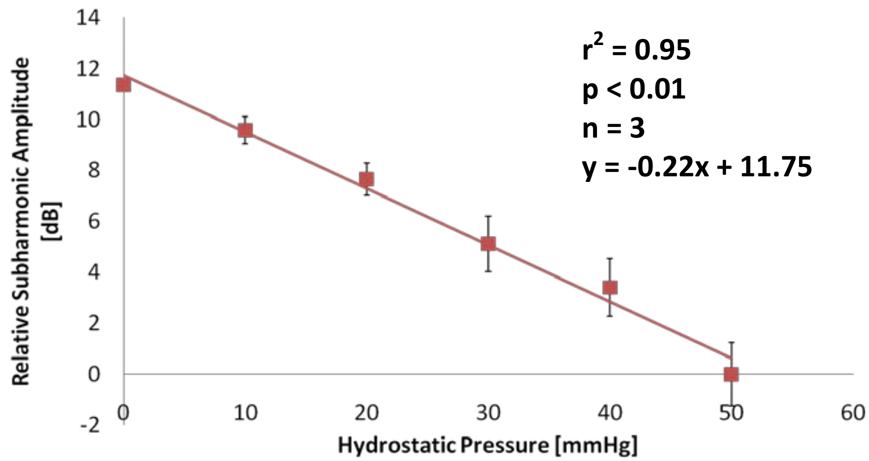

Figure 7. *Inverse linear relationship between pressure and subharmonic signal amplitude for Definity at 10 MHz and -8 dB acoustic output power (N = 3).*

and thereby the frequency ratio. For different acoustic excitation pressure levels, changing ambient pressure can either increase or decrease the subharmonic response depending on this ratio. For some range of parameters, the variation is far more complicated. This behavior is clearly at odds with the experimental observations mentioned above and is currently not well understood. These discrepancies may be due to encapsulation buckling or strain softening in describing nonlinear oscillations, specifically the subharmonic response [33]. This investigation has been published [33-34]. This constitutes the completion of tasks 1b, 1c and 1e.

In vivo experiments

Software to analyze RF data from the Sonix RP scanner has been improved and the best method to extract the subharmonic signal components from the frequency spectrum has been established. This software is applicable to RF data acquired from any tissues (including breast tumors). However, due to the availability of canine cardiac data (obtained with funds from other sources, but processed with funds from this grant), our initial work focused on cardiac SHAPE pressure estimates [32, 35-37]. Briefly, the unprocessed RF data for each accumulated pulse (Fig. 8A) was transformed to the Fourier domain and the subharmonic signal amplitude (at half the fundamental frequency – Fig. 8B) was extracted as the average signal in a 40 % bandwidth around the subharmonic frequency (i.e., here 1.25 MHz). The extracted subharmonic signals from all pulses were processed using a moving average filter to eliminate noise spikes. The range of the subharmonic signal (i.e., the difference between maximum and minimum subharmonic amplitude) was compared from each pulse contour (after eliminating excessively noisy pulses) for each incident acoustic pressure. Since the pressure tracking using microbubbles is an incident acoustic pressure dependent phenomenon, the incident acoustic pressure with maximum stable subharmonic range was then selected for LV pressure tracking; as shown in Figure 8C.

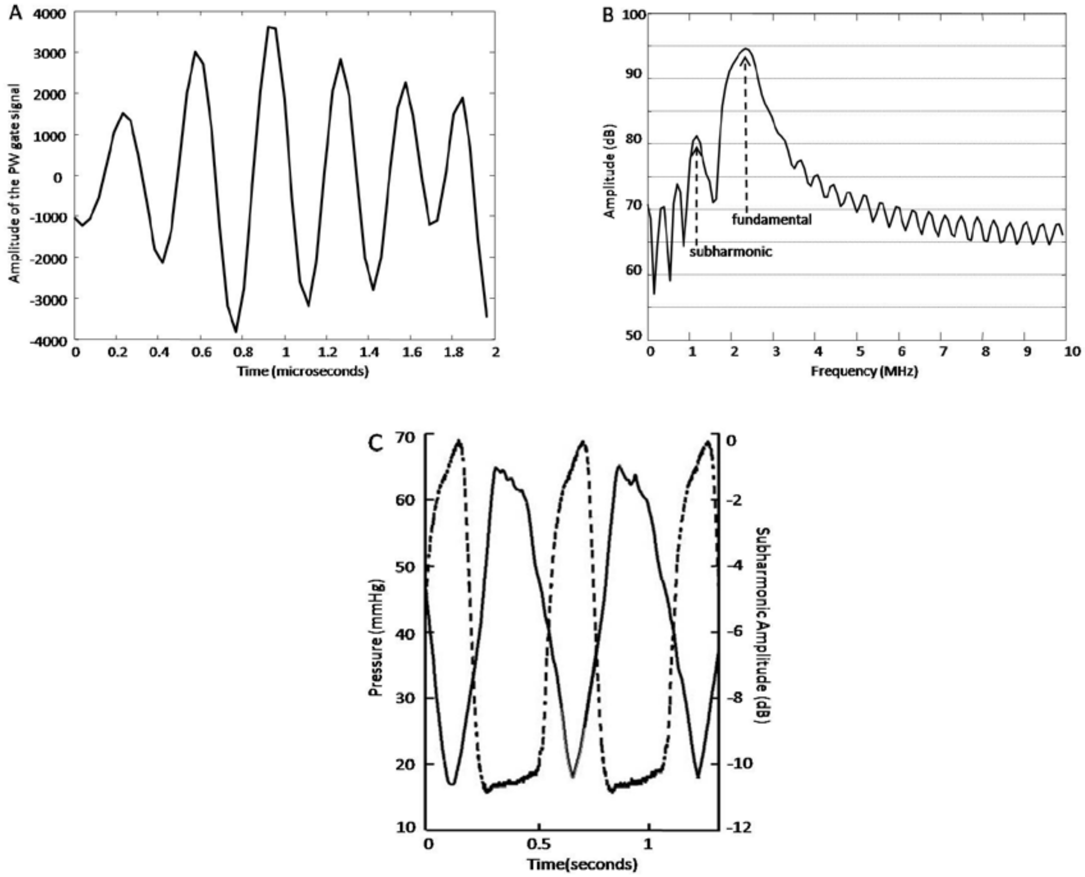

***Figure 8**: Steps involved in extracting and processing the subharmonic signal for SHAPE. A typical signal obtained with pulsed Doppler (A) and the frequency domain representation (B) of the signal in (A). The processed subharmonic signal from all the pulses (solid line) and the pressure catheter data (dotted line) are shown in (C). Note the inverse relationship between the subharmonic signal and the pressure obtained via the pressure catheter (in agreement with our previously published in vitro results).*

Results from seven canines indicate that maximum absolute errors on the order of -1.36 to 2.50 mmHg can be obtained for diastolic left ventricular pressures if the aortic pulse pressure values are known; otherwise maximum absolute errors for LV estimates compared to the reference standard were slightly larger (up to 9 mmHg) [35-37]. Moreover, estimating the peak systolic RV pressure resulted in errors of 0.0 to 3.5 mmHg [35-37]. Moreover, a patent application has been submitted to the U.S Patent Office based on these development efforts [38]. This effort represents the conclusion of task 2b.

A unique opportunity to test the Stryker pressure monitoring system and provide proof-of-concept of the use of SHAPE for estimating IFP was pursued in the Sinclair swine melanoma model. Five (5) swine were studied, but one of the swine was eliminated from the study, due to technical difficulties. The difference between the subharmonics and the IFP in tumors and their surrounding tissues was most linear for 10 MHz transmission ($r^2 \geq 0.67$; $p < 0.05$; Fig. 9) [39-40]. The difference between tissue and tumor IFP is rather large and may be caused by the sensitivity of the Stryker system to the angle between the needle and the tissue being studied (this issue is currently being investigated further). The slope from 3 out of 4 animals was very similar to each other (-0.19 ± 0.07) and to the *in* vitro slope (-0.22), while the last swine (i.e., swine 1) showed a large spread within the normal tissue IFP. In conclusion, these results provide proof of concept for the feasibility of using SHAPE as a noninvasive monitor of IFP.

Finally, the work on *in vivo* SHAPE measurements of IFP in melanoma swine [39] was selected for the final of the American Institute of Ultrasound in Medicine (AIUM) 2011 Young Investigator Award (for V. G. Halldorsdottir) and was <u>awarded FIRST place out of 90 abstracts submitted for this competition</u>.

Of the 25 rats implanted with MDA-MB-231 for the initial calaibration studies, 16 (64 %) exhibited tumor growth and 13 were successfully imaged in completion of task 3a and 3b. In the treatment groups (for days 21, 24 and 28) 60 rats received injections of the breast cancer cells into the right mammary fatpad, which resulted in 38 animals with tumors and amongst those 26 were successfully imaged. The 15 rats with tumor growth that failed the imaging study were mainly for technical reasons (the experimental software on the Sonix RP crashed occasionally). The treatment groups therefore ended up containing 8, 9 and 9 rats for 21, 24 and 28 days post-implantation, respectively. In each group there were 2 rats that were designated as control cases (i.e., they did not receive injections of paclitaxel). SHI depicted the tortuous morphology of tumor neovessels and delineated areas of necrosis better than fundamental ultrasound imaging, due to the suppression of tissue signals. However, the degree of tissue suppression was less than other *in vivo* studies undertaken by our group [31, 41-42], which was attributed to the nonlinear transfer function of the scanner.

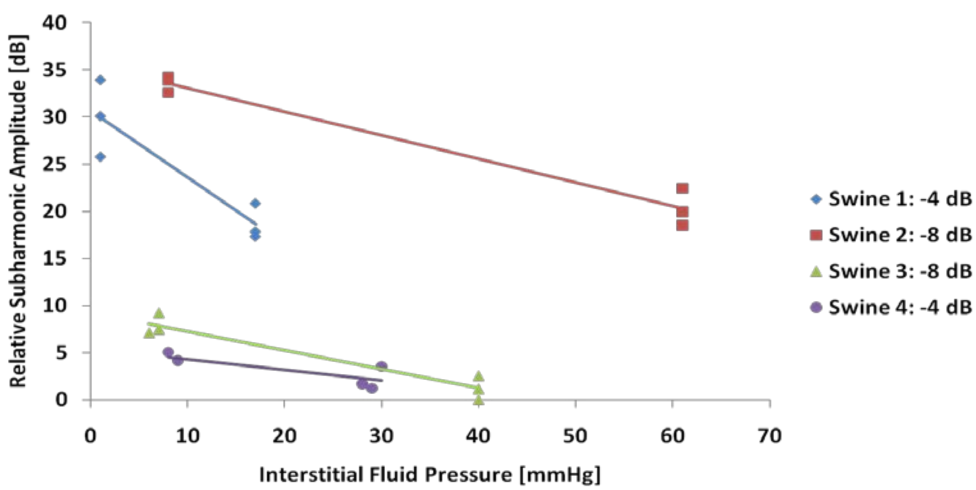

Figure 9. *In vivo measurements showing SHAPE results compared to the pressure monitor. The relative difference between tissue and tumor IFP is clearly captured by SHAPE.*

The change in tumor volume as well as in IFP (measured with the Stryker reference standard) from pre to post treatment is depicted in Figure 10. The change encountered for the control animals have also been included. For both markers the standard deviations are quite large, but for the IFP values a clear trend is seen with the IFP reducing more as time increases. However, for both tumor volume and IFP measurements there were no statistically significant differences between the control and the treatment groups ($p > 0.37$). It should be pointed out that the main analysis planned for this project - the comparisons between SHAPE and Stryker IFP measurements – is still ongoing. This is due to both the students on this project (V Halldorsdottir and A Marshall) becoming parents within the last 4 months and coupled with the issues of pregnancy, they were not able to finalize the data analysis in time. This work (under task 3d) is still ongoing.

The SHI images were rendered into maximum intensity projection (MIP) mode in order to better isolate contrast enhanced pixels from tissue background and noise signals (Fig. 11) when calculating the FV. When analyzing the immunohistochemical markers of angiogenesis, VEGF was found to vary significantly over time ($p<0.031$), while the strongest correlation determined by linear regression in this breast cancer model was between SHI and percent area stained with VEGF ($r = 0.53$; Table 1). This represents the completion of Task 3c. It should be pointed out that the results in Table 1 are based on 32 rats and involve values obtained over the entire tumor area. However, given the known tumor heterogeneity, it is very likely the averaging over the entire area will not be optimal [23]. Hence, we intend to re-analyze this data split into smaller regions of interest. Another limitation is the inherent problem in matching ultrasound images with beam-widths on the order of mm to pathology specimens cut in 5 μm sections; even though great care was taken to match the imaging planes to the pathology sections (as described above).

Finally, the work on comparing *in vivo* SHI measurements of tumor vascularity in murine xenografts to immunohistochemical markers [43] was selected for the final of the AIUM 2013 Young Investigator Award (for A. Marshall). Although placements beyond first place are not released, it should be noted that this abstract was one out of 11 selected from a pool of 111 abstracts submitted for this competition.

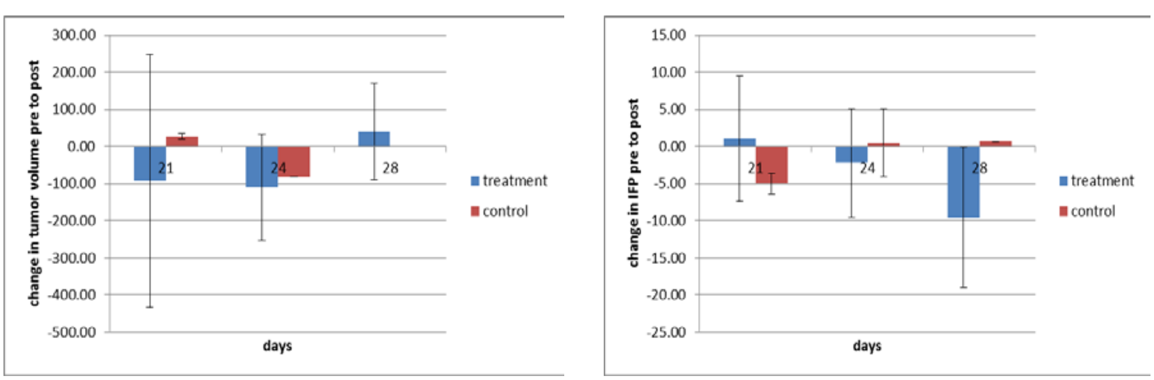

Figure 10. *The change in tumor volume (A) and IFP measurements (B) from pre to post administration of Paclitaxel. Notice how the treatment results in lower IFP values at days 24 and 28, as expected.*

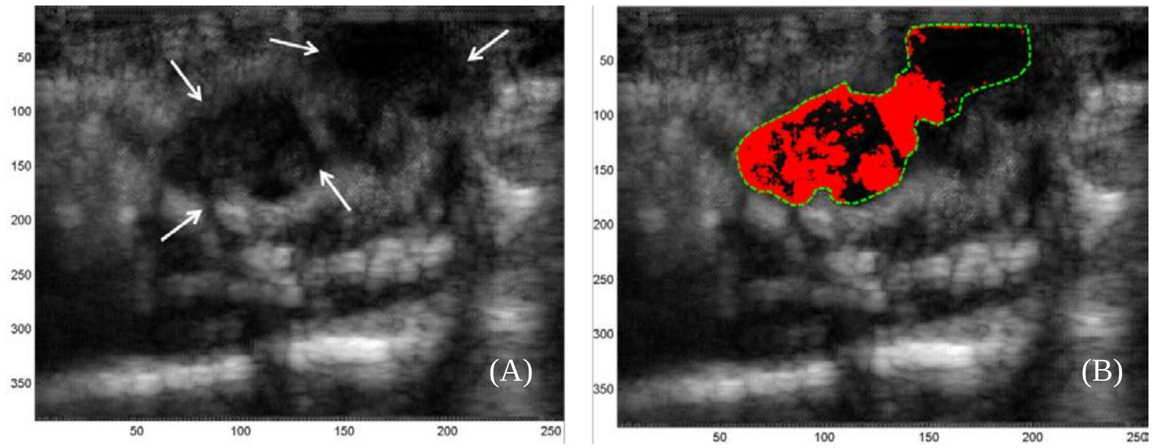

Figure 11. *Breast tumor xenograft (arrows) depicted in maximum projection intensity (MIP) SHI mode (A) and the pixels corresponding to vascularity in red within the tumor boundary (green dotted line) shown in (B).*

Table 1. Correlation between SHI and angiogenic markers in 32 rats.

	VEGF vs. SHI		**COX-2 vs. SHI**		**CD-31 vs. SHI**	
	r	**p**	**r**	**p**	**r**	**p**
Day 21 (n=11)	0.202	0.551	0.158	0.642	0.304	0.363
Day 24 (n=11)	0.529	0.094	0.134	0.692	0.114	0.737
Day 28 (n=10)	0.032	0.943	0.063	0.857	0.045	0.901
Overall (n=32)	0.032	0.890	0.071	0.689	0.071	0.689

6 KEY RESEARCH ACCOMPLISHMENTS

- SHAPE experiments were conducted with Definity and Sonazoid *in vitro* in a pressurized watertank (range: 0-50 mmHg) using the pulse-echo setup.
- SHAPE experiments were conducted *in vitro* with Definity using the Sonix RP scanner and two different probes; L14-5/38 and L9-4/38.
- Hydrostatic pressure is inversely related to the change in subharmonic amplitude ($r^2 = 0.76–0.91$, $p < 0.01$).

- A computer model to simulate the behavior of microbubbles as a function of pressure has been developed.
- SHAPE experiments were conducted *in vitro* in a new, improved water-tank.
- The maximum decrease obtained with Definity over 50 mmHg was 11.36 dB (r^2=0.95; p<0.01) at 10 MHz and -8 dB power.
- Software for processing of *in vivo* SHAPE data has been developed and optimized.
- *In vivo* proof of concept for SHAPE as a noninvasive monitor of IFP has been provided (r^2 = 0.67 – 0.96, p < 0.01).
- The L9-4 linear array has been selected for the *in vivo* studies.
- Sonix RP scanner design requirements have been developed and implemented.
- Lantheus Medical decided to support this project with 230 vials of Definity for use in the *in vivo* experiments.
- *In vivo* SHAPE data from 26 rats before and after treatment with paclitaxel have been acquired, but not yet analyzed.
- Initial data analysis indicate that SHI measures of vascularity may correlate with the expression of VEGF (r = 0.53).

7 REPORTABLE OUTCOMES

Publications - abstracts

F. Forsberg, A. Katiyar, L. M. Leodore, K. Sarkar. Noninvasive subharmonic pressure estimation: in vitro experiments and modeling. *J Ultrasound Med*, vol 28 (Suppl.), pp. S120 – S121, 2009.

F. Forsberg, V. G. Halldorsdottir, J. Dave, M. McDonald, J. B. Liu, C. Leung, K. Dickie. In vivo noninvasive cardiac subharmonic pressure estimation. *Ultrasonic Imaging,* vol. 31, pp. 45-46, 2009.

V. G. Halldorsdottir, L. Leodore, B. Cavanaugh, F. Forsberg. Pressure estimation for monitoring neoadjuvant chemotherapy of breast cancer: In vitro measurements. *Ultrasonic Imaging,* vol. 31, pp. 46, 2009.

F. Forsberg. Applications of subharmonic contrast imaging. *Ultrasound Med Biol*, vol. 35, pp. S32, 2009.

V. G. Halldorsdottir, L. M. Leodore, B. Cavanaugh, F. Forsberg. Initial *in vitro* study of US pressure measurements for monitoring neoadjuvant chemotherapy of breast cancer. *Prog. RSNA*, pp. 338, 2009.

F. Forsberg, J. Dave, V. G. Halldorsdottir, M. McDonald, J. B. Liu C. Leung, K. Dickie. Noninvasive cardiac subharmonic pressure estimation in vivo. *J Ultrasound Med*, vol 29, no 3, pp. S13, 2010.

F. Forsberg. The holy grail: ultrasound microbubbles for therapy. *J Ultrasound Med*, vol 29, no 3, pp. S17, 2010.

F. Forsberg. Subharmonic imaging and pressure estimation. *Med Phys*, vol 37, no 6, pp 3397-3398, 2010.

J. K. Dave, V. G. Halldorsdottir, J. R. Eisenbrey, J. B. Liu, F. Lin, J. H. Zhou, H. K. Wang, K. Thomenius, F Forsberg. In vivo subharmonic pressure estimation of portal hypertension in canines. *Proc IEEE US Symp,* pp. 778-781, 2010.

S. Paul, K. Sarkar, F.Forsberg. Strain-softening elasticity model of the encapsulation of an ultrasound contrast microbubble. *Am Phys Soc, Div Fluid Dynam*, http://meetings.aps.org/link/BAPS.2010.DFD.LR.1, 2010.

A. Katiyar, K. Sarkar, F.Forsberg. Subharmonic response from ultrasound contrast microbubbles for noninvasive blood pressure estimation. *Am Phys Soc*, *Div Fluid Dynam*, http://meetings.aps.org/link/BAPS.2010.DFD.HL.1, 2010.

*V. G. Halldorsdottir, J. K. Dave, J. Eisenbrey, P. Machado, J. B. Liu, D. A. Merton, B. C. Cavanaugh, F. Forsberg. Subharmonic aided pressure estimation for monitoring interstitial fluid pressure in tumors: *in vitro* and *in vivo* proof of concept. *J Ultrasound Med*, vol. 30, pp. S28, 2011.

J. Dave, V. G. Halldorsdottir, J. Eisenbrey, M. McDonald, J. B. Liu, J. Raichlen, C. Leung, K. Dickie, F. Forsberg**.** Subharmonic signals for noninvasive cardiac pressure estimation – initial *in vivo* experience. *J Ultrasound Med*, vol. 30, pp. S71 – S72, 2011.

F. Forsberg, J. K. Dave, V. G. Halldorsdottir, J. R. Eisenbrey, J. S. Raichlen, J. B. Liu, C. Miller, J. M. Gonzalez, M. E. McDonald, D. A. Merton, D. Brown, V. Navarro. On the utility of subharmonic contrast microbubble signals. *Ultrasonic Imaging*, vol. 33, pp. 65-66, 2011.

K. Sarkar, A. Katiyar, F. Forsberg. Dynamics of contrast microbubbles and their subharmonic response for noninvasive blood pressure estimation. *Ultrasonic Imaging*, vol. 33, pp. 66-67, 2011.

F. Forsberg, V. G. Halldorsdottir, B. C. Cavanaugh, P. Machado, J. B. Liu, J. Eisenbrey, J. K. Dave, D. A. Merton. Subharmonic aided pressure estimation for monitoring neoadjuvant chemotherapy of locally advanced breast cancer. *Proc Era of Hope*, pp. 595, 2011.

J. K. Dave, V. G. Halldorsdottir, J. R. Eisenbrey, J. B. Liu, M. E. McDonald, K. Dickie, C. Leung, F. Forsberg. Noninvasive estimation of dynamic pressures in vitro and in vivo using the subharmonic response from microbubbles. Proc IEEE US Symp, pp. 176-179, 2011.

J. R. Eisenbrey, J. K. Dave, V. G. Halldorsdottir, S. Park, S. Dianis, D. A. Merton, P. Machado, J. B. Liu, J. M. Gonzalez, C. Miller, K.E. Thomenius, D. B. Brown, V. Navarro, F. Forsberg. Dual grayscale and subharmonic ultrasound imaging on modified ultrasound scanner in 2 and 3D. Proc IEEE US Symp, pp. 624-627, 2011.

V. G. Halldorsdottir, J. Eisenbrey, J. K. Dave, F. Forsberg, P. Machado, B. C. Cavanaugh, D. A. Merton, J. B. Liu. Subharmonic aided pressure estimation for monitoring interstitial fluid pressure in swine melanomas: initial in vitro and in vivo results. Prog RSNA, abstract no SSA21-03, 2011.

F. Forsberg, J. R. Eisenbrey, J. K. Dave, V. G. Halldorsdottir, J. B. Liu, J. M. Gonzalez, C. Miller, P. Machado, D. A. Merton, S. Park, S. Dianis, C. L. Chalek, K.E. Thomenius, D. B. Brown, V. Navarro. Dual grayscale and subharmonic US imaging on a modified commercial scanner. Prog RSNA, abstract no LL-PHS-SU9A, 2011.

J. K. Dave, V. G. Halldorsdottir, J. Eisenbrey, F. Forsberg. Processing acoustic data from US contrast agents for ambient pressure estimation. Prog RSNA, abstract no LL-PHS-SU9B, 2011.

F. Forsberg, J. K. Dave, V. G. Halldorsdottir, J. R. Eisenbrey, J. S. Raichlen, J. B. Liu, M. E. McDonald, S. Wang, C. Leung, K. Dickie. Noninvasive cardiac pressure estimation using subharmonic microbubble signals. Prog RSNA, abstract no LL-CAS-WE6A, 2011.

J. K. Dave, V. G. Halldorsdottir, J. R. Eisenbrey, S. Park, S. Dianis, C. L. Chalek, D. A. Merton, J. B. Liu, P. Machado, K. E. Thomenius, D. B. Brown, F. Forsberg. Automated power optimization for subharmonic aided pressure estimation. J Ultrasound Med, vol. 31, pp. S44, 2012.

J. K. Dave, V. G. Halldorsdottir, J. R. Eisenbrey, J. S. Raichlen, J. B. Liu, M. E. McDonald, K. Dickie, S. Wang, C. Leung, F. Forsberg. Noninvasive right ventricular pressure estimation in vivo using the subharmonic emissions from ultrasound contrast agents Proc IEEE Int Ultrason Symp, pp. 1114-1117, 2012.

**A Marshall, VG Halldorsdottir, JK Dave, AI Forsberg, M Dahibawkar, TB Fox, JB Liu, X Hu, Y He, F Forsberg. Subharmonic imaging of angiogenesis in a murine breast cancer model. J Ultrasound Med, vol. 32, pp. S51, 2013.

A Marshall, JK Dave, F Forsberg, VG Halldorsdottir, AI Forsberg, M Dahibawkar, TB Fox, JB Liu. Comparing Immunohistochemical Markers of Angiogenesis to Subharmonic Imaging of Vascularity in a Murine Breast Cancer Model. Submitted to RSNA, 2013.

Publications – journal papers

S. Paul, A. Katiyar, K. Sarkar, D. Chatterjee, W. T. Shi, F. Forsberg. Material characterization of the encapsulation of an ultrasound contrast microbubble and its subharmonic response: strain-softening interfacial elasticity model. *J Acoust Soc Am.*, vol. 127, no. 6, pp. 3846-3857, 2010.

A. Katiyar, K. Sarkar, F. Forsberg. Modeling subharmonic response from contrast microbubbles as a function of ambient static pressure. *J Acoust Soc Am*, vol. 129, no. 4, pp. 2325 – 2335, 2011.

V. G. Halldorsdottir, J. K. Dave, L. M. Leodore, J. R. Eisenbrey, S. Park, A. L. Hall, K. Thomenius, F. Forsberg. Subharmonic contrast microbubble signals for noninvasive pressure estimation under static and dynamic flow conditions. *Ultrasonic Imaging*, vol. 33, no 3, pp. 153-164, 2011.

J. K. Dave, V. G. Halldorsdottir, J. R. Eisenbrey, J. B. Liu, M. E. McDonald, K. Dickie, C. Leung, F. Forsberg. Noninvasive estimation of dynamic pressures in vitro and in vivo using the subharmonic response from microbubbles. *IEEE Trans Ultrason, Ferroelec and Freq Control*, vol. 58, no 10, pp. 2056 - 2066, 2011.

J. R. Eisenbrey, J. K. Dave, V. G. Halldorsdottir, D. A. Merton, P. Machado,J. B. Liu, C. L. Miller, J. M. Gonzalez, S. Park, S. Dianis, C. L. Chalek, K.E. Thomenius, D. B. Brown, V. J. Navarro, F. Forsberg. Simultaneous grayscale and subharmonic ultrasound imaging on a modified commercial scanner. *Ultrasonics*, vol. 51, no. 12, pp. 890-897, 2011.

J. K. Dave, V. G. Halldorsdottir, J. R. Eisenbrey, J. S. Raichlen, J. B. Liu, M. E. McDonald, K. Dickie, S. Wang, C. Leung, F. Forsberg. Noninvasive LV pressure estimation using subharmonic emissions from microbubbles. *JACC Cardiovasc Imaging*, vol. 5, no. 1, pp. 87 – 92, 2012.

J. K. Dave, V. G. Halldorsdottir, J. R. Eisenbrey, F. Forsberg. On the processing of subharmonic signals from ultrasound contrast agents to determine ambient pressures. *Ultrason Imaging*, vol. 34, no. 2, pp. 81-92, 2012.

J. K. Dave, V. G. Halldorsdottir, J. R. Eisenbrey, J. S. Raichlen, J. B. Liu, M. E. McDonald, K. Dickie, S. Wang, C. Leung, F. Forsberg. Subharmonic microbubble emissions for noninvasively tracking right ventricular pressures. *Am J Physiol Heart Circ Physiol*, vol. 303, no. 1, pp. H126–H132, 2012.

J. K. Dave, V. G. Halldorsdottir, J. R. Eisenbrey, D. A. Merton, J. B. Liu, P. Machado, H. Zhao, S. Park, S. Dianis, C. L. Chalek, K. E. Thomenius, D. B. Brown, F. Forsberg. On the implementation of an automated acoustic output optimization algorithm for subharmonic aided pressure estimation. *Ultrasonics*, vol. 53, no. 4, pp. 880 – 888, 2013

V. G. Halldorsdottir, J. K. Dave, J. R. Eisenbrey, P. Machado, J. B. Liu, D. A. Merton, F. Forsberg. Subharmonic aided pressure estimation for monitoring interstitial fluid pressure in tumors: in vitro and in vivo proof of concept. Submitted to *Phys Med Biol*, December, 2012.

Presentations

April 2 - 5, 2009	The 54th Annual Convention of the American Institute of Ultrasound in Medicine, New York City, NY, USA. • Noninvasive subharmonic pressure estimation: in vitro experiments and modeling.
June 10 – 12, 2009	34th International Symposium on Ultrasonic Imaging and Tissue Characterization, Arlington, VA. • Pressure estimation for monitoring neoadjuvant chemotherapy of breast cancer: in vitro measurements. • In vivo noninvasive cardiac subharmonic pressure estimation.
August 30 - September 3, 2009	The 12th Congress of the World Federation for Ultrasound in Medicine and Biology, Sydney, Australia. • Applications of subharmonic contrast imaging.
October 8, 2009	QED Program, University City Science Center, Philadelphia, PA, USA. • Non-invasive pressure estimation using ultrasound.
October 22-23, 2009	24th Annual Advances in Contrast Ultrasound & ICUS Bubble Course 2009, Chicago, IL, USA. • In vivo subharmonic pressure estimation.
November 29 - December 4, 2009	The 95th Scientific Assembly and Annual Meeting of the Radiological Society of North America, Chicago, IL, USA. • Initial in vitro study of US pressure measurements for monitoring neoadjuvant chemotherapy of breast cancer.
March 25 - 28, 2010	The 55th Annual Convention of the American Institute of Ultrasound in Medicine, San Diego, CA, USA. • Noninvasive cardiac subharmonic pressure estimation in vivo. • The holy grail: ultrasound microbubbles for therapy
May 7, 2010	Spring Symposium, the Delaware Valley Chapter of the American Association of Physicists in Medicine, Philadelphia, PA. • Recent advances in ultrasound for image guided therapy.

July 18 - 22, 2010	52nd Annual Meeting of the American Association of Physicists in Medicine, Philadelphia, PA, USA. • Subharmonic imaging and pressure estimation.
September 30 - October 1, 2010	25th Annual Advances in Contrast Ultrasound & ICUS Bubble Course 2010, Chicago, IL, USA. • In vivo cardiac subharmonic pressure estimation.
October 11 - 14, 2010	IEEE 2010 International Ultrasonics Symposium, San Diego, CA, USA. • In vivo subharmonic pressure estimation of portal hypertension in canines.
November 21–23, 2010	63rd Annual Meeting of the American Physical Society, Division of Fluid Dynamics Long Beach, CA, USA. • Strain-softening elasticity model of the encapsulation of an ultrasound contrast microbubble. • Subharmonic response from ultrasound contrast microbubbles for noninvasive blood pressure estimation.
April 14 - 17, 2011	The 56th Annual Convention of the American Institute of Ultrasound in Medicine, New York City, NY, USA. • Subharmonic aided pressure estimation for monitoring interstitial fluid pressure in tumors: *in vitro* and *in vivo* proof of concept. • Subharmonic signals for noninvasive cardiac pressure estimation – initial *in vivo* experience.
May 23-27, 2011	Acostical Society of America meeting, Seattle, WA, USA. • Subharmonic response from ultrasound contrast microbubbles for noninvasive blood pressure estimation
June 13 – 15, 2011	Thirty-Sixth International Symp. on Ultrasonic Imaging and Tissue Characterization, Washington DC, USA. • On the utility of subharmonic contrast microbubble signals. • Dynamics of contrast microbubbles and their subharmonic response for noninvasive blood pressure estimation
August 2 – 5, 2011	Era of Hope, Dept of Defense Breast Cancer Research Meeting, Orlando, FL, USA. • Subharmonic aided pressure estimation for monitoring neoadjuvant chemotherapy of locally advanced breast cancer (poster).
October 18 - 21, 2011	IEEE 2011 International Ultrasonics Symposium, Orlando, FL, USA.

	• Dual grayscale and subharmonic ultrasound imaging on modified ultrasound scanner in 2 and 3D (poster).
November 27 - December 2, 2011	The 97th Scientific Assembly and Annual Meeting of the Radiological Society of North America, Chicago, IL, USA. • Subharmonic aided pressure estimation for monitoring interstitial fluid pressure in swine melanomas: initial *in vitro* and *in vivo* results. • Dual grayscale and subharmonic US imaging on a modified commercial scanner (eposter). • Processing acoustic data from US contrast agents for ambient pressure estimation (eposter). • Noninvasive cardiac pressure estimation using subharmonic microbubble signals (eposter).
November 29, 2011	QIBA Ultrasound Quantitative Biomarker Exploratory Meeting, Chicago, IL, USA. • Pressure measurements with contrast agents.
February 3, 2012	Reunion Internacional Sobre Avances en Hepatologia IV, Valladolid, Spain. • Subharmonic aided pressure estimation (SHAPE): a noninvasive technique for the measurement of fluid pressures using ultrasound contrast agents.
October 7 - 10, 2012	IEEE 2012 International Ultrasonics Symposium, Dresden, Germany. • Noninvasive right ventricular pressure estimation *in vivo* using the subharmonic emissions from ultrasound contrast agents.
April 6 - 10, 2013	The 58th Annual Convention of the American Institute of Ultrasound in Medicine, New York City, NY, USA. • Subharmonic imaging of angiogenesis in a murine breast cancer model

V. G. Halldorsdottir was selected as a finalist for the AIUM 2011 Young Investigator Award based on her work in the abstract labled * above. The competition was judged at the Annual Conference of the AIUM (in April 2011 in New York City, NY) and was awarded FIRST place out of 90 abstracts submitted for this competition.

A. Marshall was selected as a finalist for the AIUM 2013 Young Investigator Award based on his work in the abstract labled ** above. The competition was judged at the Annual Conference of the AIUM (in April 2013 in New York City, NY) and although it did not receive a first place it was one out of 11 abstracts selected from a pool of 111 submitted for this competition.

Patents
F. Forsberg, J. K. Dave, V. G. Halldorsdottir, J. R. Eisenbrey. Methods for improved selection, processing and display of subharmonic microbubble signals as pressure estimates. U.S. Patent pending 61/498,278, June, 2011.

Degrees
While no students have yet graduated based on the data acquited as part of this project, our expectation currently is that one (1) PhD and two (2) MSc's will be granted by Drexel University.

8 CONCLUSIONS

We have investigated six US contrast agents for use in SHAPE and shown that Definity (Lantheus Medical Imaging, N Billerica, MA) has an inverse linear relationship between the change in subharmonic amplitude and hydrostatic pressure ($r^2 = 0.63 – 0.95$, $p < 0.01$) over the pressure range associated with breast tumors (0 – 50 mmHg) when measured *in vitro* employing the new water-tank (with extra acoustic absorbers incorporated). This work has been partially published [15].

Our attempts to design a realistic simulation model accounting for the experimental results have been mixed and further work is ongoing. These efforts have been published [33-34]. Software for analyzing RF data from the Sonix RP scanner to produce SHAPE pressure estimates has been successfully optimized and several publications and a patent have been published or are in review [32, 35-38].

Moreover, *in vivo* proof-of-concept for SHAPE as a noninvasive monitor of IFP has been provided in 5 swine with naturally occurring melanoma. SHAPE showed excellent correlation with IFP values obtained in normal tissues and in the tumor using intra-compartmental pressure measurements with the wick-in-a-needle technique ($r^2 = 0.67$ –- 0.96, $p < 0.01$) [39-40]. The work on *in vivo* SHAPE measurements of IFP was selected for the final of the American Institute of Ultrasound in Medicine (AIUM) 2011 Young Investigator Award (for V. G. Halldorsdottir) and was <u>awarded FIRST place out of 90 abstracts submitted for this competition</u> [39].

Due to the delay caused by the *in vitro* experiments and some personal issues over the summer of 2012, the project was granted a 16 months no cost extension during which task 3 was to be completed. However, it took markedly longer than expected (over 6 months) to arrive at a stable and consistent level of cell growth for the MDA-MB-231 breast cancer cells, which also produced tumor growth *in vivo*. During this time period we developed an automated AO optimization algorithm to identify the AO level eliciting growth stage subharmonic signals [21]. In total, ninety-seven (97) female, nude rats were implanted with MDA-MB-231 cells and 51 animals were successfully studied with SHI and SHAPE 21, 24 or 28 days after tumor inoculation. However, the comparisons between SHAPE and Stryker IFP measurements have yet to be completely finalized.

The SHI images of tumor vascularity were compared to immunohistochemical markers of angiogenesis (CD31, COX-2 and VEGF). The strongest correlation determined by linear regression in this breast cancer model was between SHI and percent area stained with VEGF ($r = 0.53$; Table 1). However, we are in the process of re-analyzing this data over smaller ROI's to better account for tumor heterogeneity. Nonetheless, this work on comparing *in vivo* SHI measurements of tumor vascularity in murine was selected for the final of the AIUM 2013 Young Investigator Award (for A. Marshall) as one out of 11 selected from a pool of 111 abstracts submitted for this competition [43].

Given the results above and the fact that our group has published twenty-seven (27) abstracts at national and international conferences as well as ten (10) peer-reviewed papers and one (1) patent application in the almost 4 years the original BRCP award have been underway, we submitted an IDEA Expansion proposal to the BRCP. This proposal build on the work achieved in our prior BCRP awards by performing the all important translation of these methods towards clinical feasibility by conducting a first-in-humans clinical trial of 3D SHAPE in women undergoing neoadjuvant chemotherapy. This proposal was funded in 2012 and is currently underway.

In summary, tasks 1 and 2 have been completed while task 3 is ongoing (due to the parental issues involving the 2 students on this project).

9 REFERENCES

1. Favret AM, et al., Locally Advanced Breast Cancer: Is Surgery Necessary? *The Breast Journal*, 2001. **7**(2): p. 131-137.
2. Kaufmann M, et al., International Expert Panel on the Use of Primary (Preoperative) Systemic Treatment of Operable Breast Cancer: Review and Recommendations. *J Clin Oncol*, 2003. **21**(13): p. 2600-2608.
3. Guarneri V, et al. Primary systemic therapy for operable breast cancer: A review of clinical trials and perspectives. *Cancer Letters*, 2007. **248**(2): p. 175-185.
4. Esteva, FJ, Hortobagyi GN, Integration of Systemic Chemotherapy in the Management of Primary Breast Cancer. *Oncologist*, 1998. **3**(5): p. 300-313.
5. Waljee JF, Newman LA, Neoadjuvant Systemic Therapy and the Surgical Management of Breast Cancer. *Surgical Clinics of North America*, 2007. **87**(2): p. 399-415.
6. McMasters KM, Hunt KK, Neoadjuvant Chemotherapy, Locally Advanced Breast Cancer, and Quality of Life. *J Clin Oncol*, 1999. **17**(2): p. 441-.
7. Mauri D., Pavlidis N, and Ioannidis JPA, Neoadjuvant Versus Adjuvant Systemic Treatment in Breast Cancer: A Meta-Analysis. *J. Natl. Cancer Inst*., 2005. **97**(3): p. 188-194.
8. Heldin CH, et al., High interstitial fluid pressure - an obstacle in cancer therapy. *Nat Rev Cancer*, 2004. **4**(10): p. 806-13.
9. Less JR, et al., Interstitial hypertension in human breast and colorectal tumors. *Cancer Res*, 1992. **52**(22): p. 6371-4.

10. Taghian AG, et al., Paclitaxel Decreases the Interstitial Fluid Pressure and Improves Oxygenation in Breast Cancers in Patients Treated With Neoadjuvant Chemotherapy: Clinical Implications. *J Clin Oncol*, 2005. **23**(9): p. 1951-1961.
11. Milosevic M, et al., Interstitial fluid pressure predicts survival in patients with cervix cancer independent of clinical prognostic factors and tumor oxygen measurements. *Cancer Res*, 2001. **61**(17): p. 6400-5.
12. Goldberg BB, Liu JB, Forsberg F, Ultrasound contrast agents: A review. *Ultrasound Med Biol*, 1994. **20**(4): p. 319-333.
13. Shi WT, Forsberg F, et al., Pressure dependence of subharmonic signals from contrast microbubbles. *Ultrasound Med Biol*, 1999. **25**(2): p. 275-283.
14. Sarkar K, Shi WT, Chatterjee D, Forsberg F. Characterization of ultrasound contrast microbubbles using in vitro experiments and viscous and viscoelastic interface models for encapsulation. *J Acoust Soc Am*, **118**:539-550, 2005.
15. Halldorsdottir VG, Dave JK, Leodore LM,et al. Subharmonic contrast microbubble signals for noninvasive pressure estimation under static and dynamic flow conditions. *Ultrasonic Imaging*, 2011; **33:**153-164.
16. Yudina A, Lepetit-Coiffé M, Moonen CT. Evaluation of the temporal window for drug delivery following ultrasound-mediated membrane permeability enhancement. *Mol Imaging Biol*. 2011; **13**:239-249. [PMID: 20521134.]
17. Merz M, Komljenovic D, Semmler W, Bäuerle T. Quantitative contrast-enhanced ultrasound for imaging antiangiogenic treatment response in experimental osteolytic breast cancer bone metastases. *Invest Radiol*. 2012; **47**:422-429. [PMID: 22659593].
18. Jun YJ, Jadhav VB, Min JH, et al. Stable and efficient delivery of docetaxel by micelle-encapsulation using a tripodal cyclotriphosphazene amphiphile. *Int J Pharm.* 2012; **422**:374-380. [PMID: 22079718].
19. Li S, Goins B, Phillips WT, Saenz M, Otto PM, Bao A. Post-lumpectomy intracavitary retention and lymph node targeting of (^{99}m)Tc-encapsulated liposomes in nude rats with breast cancer xenograft. *Breast Cancer Res Treat.* 2011; **130**:97-107. [PMID: 21181436].
20. Zhao R, Gao F, Hanscom M, Goldman ID. A prominent low-pH methotrexate transport activity in human solid tumors: contribution to the preservation of methotrexate pharmacologic activity in HeLa cells lacking the reduced folate carrier. *Clin Cancer Res*. 2004; **10**:718-727. [PMID: 14760095].
21. Dave JK, Halldorsdottir VG, Eisenbrey JR, Merton DA, Liu JB, Machado P, Zhao H, Park S, Dianis S, Chalek CL, Thomenius KE, Brown DB, Forsberg F. On the implementation of an automated acoustic output optimization algorithm for subharmonic aided pressure estimation. *Ultrasonics*; 2013; **53**:880-888. [PMID: 23347593].
22. Kim SC, Kim DW, Shim YH, Bang JS, Oh HS, Wan Kim S, Seo MH. In vivo evaluation of polymeric micellar paclitaxel formulation: toxicity and efficacy. *J Control Release;* 2001; **72**:191-202. [PMID: 11389998].
23. Forsberg F, Kuruvilla B, Pascua MB, Chaudhari MH, Merton DA, Palazzo JP, Goldberg BB. Comparing contrast-enhanced color flow imaging and pathological measures of breast lesion vascularity. *Ultrasound Med Biol*. 2008; **34**:1365-1372. [PMID: 18436369].

24. Makrilia N, Lappa T, Xyla V, Nikolaidis I, Syrigos K. The role of angiogenesis in solid tumours: an overview. *Eur J Intern Med*, 2009; **20**:663-671.
25. Li WW. Tumor angiogenesis: molecular pathology, therapeutic targeting, and imaging. *Acad Radiol*, 2000; **7:**800-811.
26. Bremnes RM, Camps C, Sirera R. Angiogenesis in non-small cell lung cancer: The prognostic impact of neoangiogenesis and the cytokines VEGF and bFGF in tumours and bloo. *Lung Canc*, 2006; **51:**143-158.
27. Ferrara N. Role of vascular endothelial growth factor in the regulation of angiogenesis. *Kidney Intl*, 1999; **56:**794-814.
28. Denkert C, Köbel M, Berger S, Siegert A, Leclere A, Trefzer U, Hauptmann S. Expression of cyclooxygenase 2 in human malignant melanoma. *Cancer Res*, 2001; **61:**303-308.
29. Xu XC. COX-2 inhibitors in cancer treatment and prevention, a recent development. *Anti-Cancer Drugs*, 2002; **13:**127-137.
30. Newman PJ. The biology of PECAM-1. *J Clin Invest*, 1997: **99:**3-8.
31. Eisenbrey JE, Dave JK, Halldorsdottir VG, et al. Simultaneous grayscale and subharmonic ultrasound imaging on a modified commercial scanner. *Ultrasonics*, 2011. **51**(12): p. 890-897.
32. Dave JK, Halldorsdottir VG, Eisenbrey JR, et al. Noninvasive estimation of dynamic pressures in vitro and in vivo using the subharmonic response from microbubbles. *IEEE Trans Ultrason, Ferroelec and Freq Control*, 2011; 58: 2056 - 2066.
33. Paul S, Katiyar A, Sarkar K, Chatterjee D, Shi WT, Forsberg F. Material characterization of the encapsulation of an ultrasound contrast microbubble and its subharmonic response: strain-softening interfacial elasticity model. *J Acoust Soc Am.*, 2010. **127**: 3846-3857.
34. Katiyar A, Sarkar K, Forsberg F. Modeling subharmonic response from contrast microbubbles as a function of ambient static pressure. *J Acoust Soc Am,* 2011. **129**:2325 – 2335.
35. Dave JK, Halldorsdottir VG, Eisenbrey JR, et al. Noninvasive LV pressure estimation using subharmonic emissions from microbubbles. *JACC Cardiovasc Imaging*, 2012; **5**: 87 – 92.
36. Dave JK, Halldorsdottir VG, Eisenbrey JR, Forsberg F. On the processing of subharmonic signals from ultrasound contrast agents to determine ambient pressures. *Ultrason Imaging*, 2012; **34**:81-92.
37. Dave JK, Halldorsdottir VG, Eisenbrey JR, et al. Subharmonic microbubble emissions for noninvasively tracking right ventricular pressures. *Am J Physiol Heart Circ Physiol*, 2112; **303**:H126–H132.
38. Forsberg F, Dave JK, Halldorsdottir VG, Eisenbrey JR. Methods for improved selection, processing and display of subharmonic microbubble signals as pressure estimates. *U.S. Patent pending 61/498,278*, June, 2011.
39. Halldorsdottir VG, Dave JK, Eisenbrey J, Machado P, Liu JB, Merton DA, Cavanaugh BC, Forsberg F. Subharmonic aided pressure estimation for monitoring interstitial fluid pressure in tumors: in vitro and in vivo proof of concept (abstract). *J Ultrasound Med*, 2011; **30**:S28.

40. Halldorsdottir VG, Dave JK, Eisenbrey J, Machado P, Liu JB, Merton DA, Forsberg F. Subharmonic aided pressure estimation for monitoring interstitial fluid pressure in tumors: in vitro and in vivo proof of concept. Submitted to *Phys Med Biol*, December, 2012.
41. Forsberg F, Liu JB, Shi WT, Ro R, Lipcan KJ, Deng X, Hall AL. In vivo perfusion estimation using subharmonic contrast microbubble signals. *J Ultrasound Med*, 2006; **25**:15-21.
42. Forsberg F, Piccoli CW, Merton DA, Palazzo JP, Hall AL. Breast lesions: imaging with contrast-enhanced subharmonic US - initial experience. *Radiology*, 2007; **244:**718-726.
43. Marshall A, Halldorsdottir VG, Dave JK, Forsberg AI, Dahibawkar M, Fox TB, Liu JB, Hu X, He Y, Forsberg F. Subharmonic imaging of angiogenesis in a murine breast cancer model (abstract). *J Ultrasound Med*, 2013; **32:**S51.

Appendix I

The Statement of Work from the original proposal:

Objective 1
Task 1: Computer modeling and *in vitro* experiments (months 1 - 6)

a. Construct an *in vitro* experimental pulse-echo system for investigating the effect of hydrostatic pressure variations on contrast microbubbles and measuring the resulting changes in backscattering (Month 1).
b. Design and modify numerical codes for a theoretical model describing the dynamics of contrast microbubbles under different pressure conditions (Months 1 - 3).
c. Calculate the behavior of individual contrast microbubble and the collective behavior of contrast microbubble populations (Months 3 - 6).
d. Measure changes in backscattered fundamental, second and subharmonic signals for different contrast agents as a function of pressure (Months 2 - 6).
e. Predict optimal contrast agents for SHAPE according to the numerical simulations (Month 6).
f. Select optimal contrast agent(s) for SHI and SHAPE. The selection will mainly be based on experimental measurements (Month 6).

Objectives 2 - 3
Task 2: Design and implementation of SHAPE on a commercial US scanner (months 7 - 12)

a. Optimize SHI and SHAPE, based on *in vitro* measurements and simulations using the actual parameters of the designated transducers (Months 7 – 8).
b. Modify a state-of-the-art US imaging system (the Sonix RP) to incorporate the SHI contrast imaging modality and to perform SHAPE (Months 8 - 10).
c. Evaluate the new imaging modality and SHAPE in an *in vitro* phantom using the modified US scanner (Months 11 - 12).
d. Prepare regulatory review and obtain approval for animal studies (Months 9 - 12).

Objectives 3 - 5
Task 3: Animal experiments, data collection and analysis (months 13- 36)

a. Create and grow breast tumors by implanting one of three human breast cancer cell lines (SKBR3, BT474 or MCF-7) into the mammary fat pad of athymic, nude rats (Months 13 - 34).
b. Calibrate *in vivo* SHAPE results based on IFP measurements obtained with the intra-compartmental pressure monitor in 21 nude rats. Three groups (one per cell line) of 7 rats with breast tumors implanted will be studied (months 14 - 16).

c. Produce and evaluate the ability of SHI to depict normal vascularity as well as breast tumor angiogenesis in human xenografts implanted in nude rats compared to CD31 stained specimens (Months 17 - 34).
d. Validate the clinical potential of SHAPE as a therapy monitoring tool by studying 180 human xenograft breast tumors in nude rats (42 normal rats and 138 after administration of a chemotherapy agent paclitaxel) and comparing results to intra-compartmental pressure measurements (months 17 - 34).
e. Perform statistical analyses and write final report (months 34 - 36).